Combustion and Flame 263 (2024) 113385

Contents lists available at ScienceDirect

Combustion and Flame

journal homepage: www.sciencedirect.com/journal/combustion-and-flame

Ignition characteristics of single coal particles under ammonia co-firing conditions

Chenlin Chen, Zhihua Wang *, Yong He, Wubin Weng, Kefa Cen

State Key Laboratory of Clean Energy Utilization, Zhejiang University, Hangzhou 310027, PR China

ARTICLE INFO

Keywords:
Ammonia
Coal
Single particle
Chemiluminescence
Ignition characteristics

ABSTRACT

To meet the goal of an international carbon-neutral framework, the promotion of clean coal utilization occupies a vital position in reducing greenhouse gas emissions. Ammonia co-firing is considered as a potential strategy for future power generation to reduce fossil energy consumptions, soot, CO_2 emissions, and hydrocarbon pollutants. In the present work, the ignition characteristics of single coal particles under ammonia (NH_3) co-firing conditions were investigated. Particles were injected with NH_3 or N_2 into a hot flue gas environment at 1550 K generated by a CH_4-fired Hencken burner. Temporally resolved images of CH* chemiluminescence and char thermal radiation were captured. Combining the signal profiles, ignition modes and characteristic times of single burning particles were studied with different coal types, carrying atmospheres, and O_2 contents. When the carrier gas was replaced by NH_3 atmosphere, the ignition delay time of all coal particles was greatly shortened, and the time interval from ignition to peak, as well as the combustible component burnout time, were both lengthened due to the promoted devolatilization and combustion reaction rates of coal particles caused by the NH_3 flame. Concerning the ignition mode in the NH_3-blended cases, the homogeneous ignition behaviors of the lignite particles were further enhanced, while the bituminous particles transitioned to the homogeneous-heterogeneous united ignition mode. As the O_2 content in the flue gas increased, the ignition of all coal particles was advanced monotonously, and the chemiluminescence became more intense in both N_2 and NH_3 atmospheres.

1. Introduction

The clean utilization of fossil fuels and the realization of a carbon-neutral society have become worldwide consensus in recent years. Since coal will still play important roles for many years due to its abundant reserves and cheap price, particularly in the developing countries, the carbon emission reduction nowadays from coal combustion is still great challenging. Ammonia, a zero-carbon fuel with high energy density and low storage & transportation cost, is considered to be a promising renewable substantial fuel that can be co-fired in existing coal fired furnaces or boilers for heat and power supply [1] gradually replace coal. Co-firing of ammonia with coal requires less retrofit and is especially attractive for existing thermal power stations. The ammonia supply system can be combined with the existing SCR/SNCR denitration technologies. As an efficient way to reduce carbon dioxide at source, the ammonia/coal co-firing strategy receives growing attention in both academic and industrial communities. For commercial large-scale industry systems, Chugoku Electric Power confirmed that the ammonia/coal co-firing technology can be applied in commercial operations to reduce greenhouse gas emissions in Japan's Mizushima power plant unit 2 (156 MW output) [2]. JERA Co. plans to introduce ammonia combustion technology to coal-fired power plants by 2040. JERA Co. and IHI Co. announced to demonstrate 20 % ammonia co-firing technology in a 1000 MW-class unit of the Hekinan power plant [3]. China Energy Investment Co., Ltd constructed a 40 MWth ammonia blending coal-fired boiler system. The testing system has realized the ammonia/coal mixed combustion with an ammonia blending ratio of 0–25 % and verified the feasibility of ammonia/coal co-firing technology on the industrial level [4].

In order to fundamentally understand the ammonia/coal co-firing process, Xia et al. [5,6] examined the characteristics of turbulent spherical flame propagation of the ammonia and pulverized coal co-firing process in a constant-volume chamber. The experimental data indicated that the spherical propagation velocity of the ammonia/coal flame was faster than that of coal burning, regardless of the ammonia-oxidizer equivalent ratio. Zhang et al. [7] studied the effect of the NH_3 co-firing rate on the combustion characteristics using the numerical simulation method, which showed a significant influence of the

* Corresponding author.
E-mail address: wangzh@zju.edu.cn (Z. Wang).

https://doi.org/10.1016/j.combustflame.2024.113385
Received 16 June 2023; Received in revised form 24 January 2024; Accepted 22 February 2024
Available online 27 February 2024

NH_3 co-firing rate on the flame shape. Once NH_3 co-firing rate exceeds 40%, the internal recirculation zone is completely penetrated by high-velocity NH_3 stream, leading to a long flame shape and much unreacted NH_3 leakage downstream. Takuma et al. [8] evaluated the characteristics of NH_3/coal co-firing with different injection methods in a bench-scale 1.2 MW coal-fired furnace. Researchers from the Korea Institute of Energy Research [9] conducted a preliminary experiment to observe the characteristics of ammonia-coal co-fired flame for coal-fired boiler applications and realized flame visualization for 30 % NH_3 and 70 % coal combustion in burner types of 5 kW thermal capacity. The ammonia-coal flame showed a longer shape than when gaseous ammonia was burned alone and it is considered to be the result of taking longer time for volatile matter and char combustion processes. Takamasa et al. [10] reported that ammonia addition could cause the deterioration of ignition performance for pulverized coal and the deviation of the ignition position of the flame in the boiler.

Ignition is one of the most important characteristics of fuel combustion process. Ammonia, as a gaseous fuel, has distinct ignition and combustion characteristics from coal. When coal particles are co-fired with ammonia, the gas phase ammonia is considered to ignite prior to coal, originating high-temperature environment surrounding the coal particles. As rapidly heated, the volatiles release of the pulverized coal will be promoted and the ignition and combustion processes will be accelerated. Hence, the critical scientific issue of ammonia/coal co-firing is supposed to be the gas-gas homogenous and gas-solid heterogeneous ignition mechanisms. However, to the authors' best knowledge, the studies on the ignition of coal under ammonia co-firing conditions are scarce. Considering the investigation of the ignition of single coal particles can explore more fundamental knowledge, in the present work, the ignition and combustion characteristics of single coal particles under ammonia co-firing conditions will be experimentally studied.

Studies focusing on the combustion processes of single fuel particles have been carried out for over four decades and nowadays, the study is still one of the most important stages in various fundamental coal research techniques [11]. Molina and Shaddix [12,13] investigated the ignition and devolatilization characteristics of pulverized coal particles in N_2 and CO_2 environments at 1700 K, and Bai et al. [14] evaluated the combustion characteristics of single coal particles in terms of particle size, shape, surface roughness, rotation frequency. Khatami and Levendis [15–22] explored the combustion behaviors of a series of single coal particles using high-speed cinematography and three-color pyrometry in a drop tube furnace (DTF) with optical access. Kops et al. [23] evaluated the effect of steam addition on the ignition delay times (IDT) of single coal particles in a DTF under air condition by high-speed cinematography, which indicated that the addition of steam could shorten the IDT of the particles because of the steam gasification reactions producing highly flammable species. Köser et al. [24] applied the laser-induced fluorescence (LIF) method of OH radicals on single coal particles to study the ignition and volatile combustion behaviors. Yuan et al. [25–27] used CH* chemiluminescence and three-color pyrometry to observe the ignition and devolatilization process of pulverized coal particle streams and concluded the transition behavior from heterogeneous ignition to homogeneous ignition. Qi et al. [28] obtained ignition and volatile combustion processes of single biomass and coal particles in N_2/O_2 and CO_2/O_2 environments with the temporally resolved CH* chemiluminescence method, which is regarded as an unambiguous indicator of the occurrence of volatile combustion [29,30].

In this work, we acquired the temporally resolved images of CH* chemiluminescence and char thermal radiation in ammonia/coal single particle flames by an ICCD camera equipped with 430 and 850 nm bandpass filters. Particles were carried by N_2 or NH_3 flows and injected into the hot flue gas environment generated by a CH_4-fired Hencken burner. Based on the images of CH* chemiluminescence and char thermal radiation, the ignition modes and characteristic times (including ignition delay time, the interval from ignition to peak, combustible component burnout time, etc.) of the single coal particles under different conditions (coal types, N_2 or NH_3 atmospheres, O_2 contents) are analyzed and discussed.

2. Experimental methodology

2.1. Experimental setup

As shown in Fig. 1, the ammonia/coal single particle combustion experiments were carried out in a Hencken-type flat flame burner, which consists of 600 steel tubes (I.D. 0.8 mm) inserted into a circular honeycomb plate (diameter of 60 mm). Detailed structure parameters were illustrated in our previous publication [28]. The burner chamber consists of a lower fuel gas supply part (CH_4) and an upper oxidant supply part (Air+O_2). The 600 steel tubes are connected to the fuel gas supply part and small diffusion flames are established at the tips. Single coal particles were carried by the primary stream (N_2/NH_3, flow rate at 80 mL/min) and injected into the hot environment through the central tube (I.D. 1.5 mm). A quartz shroud (I.D. 60 mm, height of 150 mm, and thickness of 3 mm) is mounted above the burner to avoid contamination of the hot flue gas by the ambient air while allowing for optical access.

The image acquisition system is presented in Fig. 2, which mainly consists of an emICCD camera (PI-MAX 4: 512EM) with two optical filters, a signal amplifier, a DG535, a FY6900 signal generator and a diaphragm. A steady 515 nm green laser beam generated by a laser diode was placed at the height of 2 mm above the central tube through where the coal particles were injected upward into the hot flue gas environment. The laser beam was shone on a photodiode (PD) abidingly. Once the coal particles passed through the laser beam, the intensity of the light collected by the PD declined rapidly, which simultaneously induced a tiny drop of the PD voltage output. After being amplified, the voltage signal was sent to a DG535 and then triggered the signal generator, which produced a series of continuous pulses with time intervals of 4 ms to control the ICCD camera. The camera was set to the on-CCD mode with the gate width (i.e. single exposure time) of 500 μs. The image doubler (LAVISION, VZ-image doubler) in front of the camera was equipped with two bandpass filters centered at 430 nm (Andover, bandwidth 10 nm) and 850 nm (Thorlabs, bandwidth 40 nm). The CH* chemiluminescence and char thermal radiation signal were acquired synchronously to realize the spectral resolution of the single particle combustion. The image regions were set as 10×60 mm^2 with a spatial resolution of ~137 μm per pixel. Through multiple exposure, a series of signal from coal particles can be obtained like the results from Fig 1(b). Through the height and jet velocity, the ignition delay time can be obtained. Meanwhile, to recognize the NH_3 flame, a 630 nm bandpass filter (Andover, bandwidth 10 nm) was used to capture the NH_2* chemiluminescence.

2.2. Coal properties and test conditions

This study investigated four kinds of typical coals: lignite from Ximeng (XM), bituminous from Inner Mongolia (IM) and Zhundong (ZD), and anthracite from Gongyi (GY). The proximate and ultimate analysis results are listed in Table 1. Before each test, the coal particles were sieved to 120~150 μm and dried at 105 ^oC for 3 h.

As shown in Table 2, the O_2 concentration of the flue gas was varied among 10 %, 20 %, and 30 %, while the temperature and average velocity at the burner exit were kept at ~1550 K and ~0.88 m/s, respectively. Pure N_2 and ammonia blended one (10 % NH_3 + 90 % N_2), abbreviated as N_2 and NH_3 atmospheres, were used as central particles carrying gases with a flow rate of 80 mL/min.

3. Results and discussion

To prove that the chemiluminescence signals acquired by the 430 nm bandpass filter is derived from CH* radicals, a high-precision spectrometer (Princeton Instruments, Acton SP2300) in 1200 lines/mm

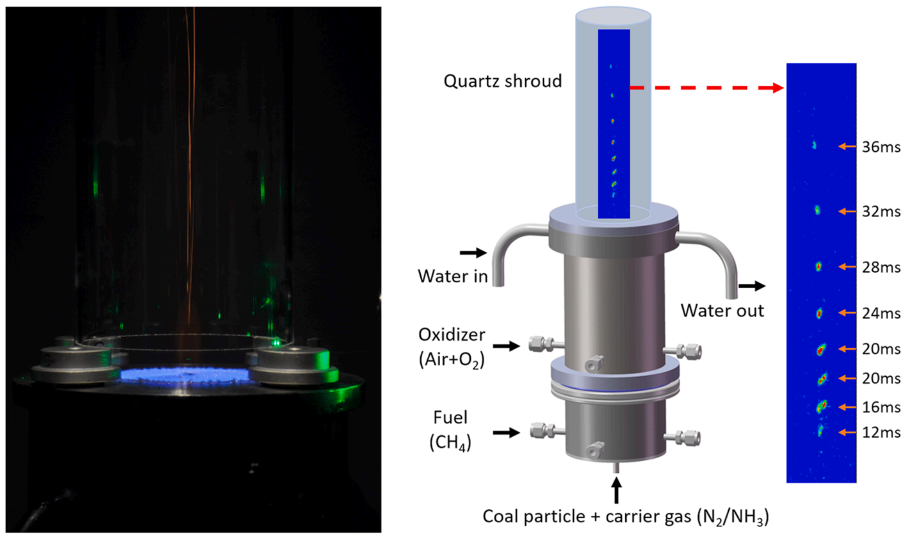

Fig. 1. Schematic of the ammonia/coal single particle combustion system. (a) Flame photo; (b) Hencken burner structure and image of CH* chemiluminescence.

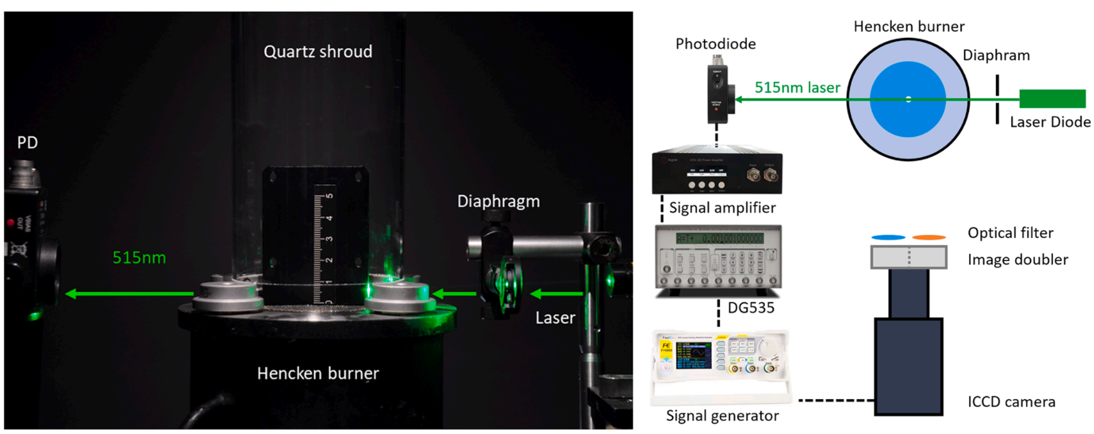

Fig. 2. Schematic of the experimental setup. (a) Photo of the laser path; (b) Synchronous trigger and optical measurement system.

Table 1
Proximate and ultimate analysis of the coal samples.

Coal	Proximate analysis (wt%)				$Q_{net,ad}$ (MJ/kg)	Ultimate analysis (wt%)				
	M_{ad}	A_{ad}	V_{ad}	FC_{ad}		C_{ad}	H_{ad}	N_{ad}	$S_{t,ad}$	O_{ad}
XM	4.50	15.47	37.90	42.13	21.95	56.00	3.55	0.97	0.54	18.97
IM	3.35	8.37	31.46	56.82	27.63	69.50	3.71	1.03	0.31	13.73
ZD	4.48	5.84	30.31	59.37	26.10	68.07	3.08	0.67	0.48	17.38
GY	2.00	9.28	7.09	81.63	31.51	80.35	2.96	1.05	0.34	4.02

Note: ad, on air-dried basis; M, moisture content; A, ash content; V, volatile content; FC, fixed carbon; Q_{net}, low heating value; S_t, total Sulphur.

grating mode was used to analyze the signals. We obtained the high-resolution chemiluminescence spectrograms of the single particle combustion process and compared them with the spectral structure of CH* characteristic peak at 431 nm from the LIFBASE database, as shown in Fig. 3 (taking XM-coal for example). It can demonstrate from the well-matched line shape that the characteristic signal at 430 nm of single particle ignition came from the intermediate radical CH* produced by the combustion of volatile fraction (C_mH_n). Combined with the filter transmittance curve, we can discover that the bandpass filter eliminated most of the ground noises of broadband signals, such as soot and coke radiation. It can ensure less interference to the wanted CH* signal and negligible influence on the ignition mode or characteristic time.

3.1. Images of ammonia/coal single particle ignition

The temporally resolved images of CH* chemiluminescence and char thermal radiation and the corresponding signal intensity profile with the variation of residence time for typical single-particle coal combustion processs are shown in Fig. 4. The O_2 content of the background flue gas was 20 vol.%, and the pulverized coal was carried by N_2 (1~4) and NH_3 (5~8), respectively. Generally, the ignition modes of fuel particles are identified into two modes [28]: (i) homogeneous ignition mode, where the gas-phase volatiles combustion take place in an enveloping flame, prior to heterogeneous oxidation of the char; and (ii) heterogeneous ignition mode, where particles ignite heterogeneously and the combustion of the volatiles and char take place simultaneously. In this work, the typical criterion of the ignition mode is identified by the transition

Table 2
Test conditions for each experiment.

Case	Coal type	Carrier gas composition	O_2 content in flue gas (%)	Outlet velocity (m/s)	Average temperature (K)
1	XM	N_2	10/20/30	0.88	1550
2	IM	N_2	10/20/30	0.88	1550
3	ZD	N_2	10/20/30	0.88	1550
4	GY	N_2	10/20/30	0.88	1550
5	XM	10 % NH_3 + 90 % N_2	10/20/30	0.88	1550
6	IM	10 % NH_3 + 90 % N_2	10/20/30	0.88	1550
7	ZD	10 % NH_3 + 90 % N_2	10/20/30	0.88	1550
8	GY	10 % NH_3 + 90 % N_2	10/20/30	0.88	1550

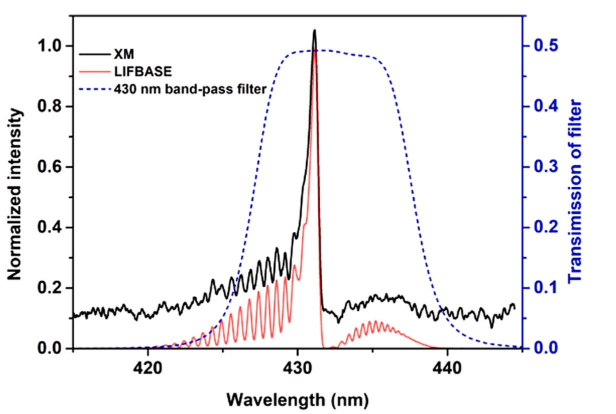

Fig. 3. Experimental spectra centered at 430 nm and CH* chemiluminescence spectrum simulation based on the LIFBASE database.

region of signal sudden drop in the image. Particles burning in two phases (volatiles flame and char combustion) with a distinguishable CH* intensity dropping region are defined as homogeneous ignition, where the volatile flames are highly sooty and luminous with soot contrails while the char combustion last longer and sparkle weaker. As for particles burning in one phase with no volatile trails or condensed phase matters are considered as heterogeneous ignition mode.

As seen from the left side of Fig. 4, when the single particle of XM lignite entered the hot environment, it was heated up rapidly, and the devolatilization reaction occurred. The CH* signal appeared at 24 ms when the homogeneous ignition began. The flame diameter of the volatile gas is about eight times that of the original particle size. As the particle temperature rose and O_2 diffused to the particle surface, the heterogeneous char combustion occurred at 44 ms (above the yellow dotted line) with the continuous release of residual volatiles in the particle [28]. However, as bituminous coal with relatively low volatile content, IM-coal and ZD-coal devolatilization rates are slower than XM-coal. Volatile matter oxidizes rapidly and cannot enrich. There are no obvious transition areas between the upper and lower part of the images, suggesting the occurrence of heterogeneous ignition, followed by the simultaneous combustion of the volatiles and char. Different from the above three types of coal, the CH* signal intensity of GY-coal cannot be detected during the single particle ignition process. Due to the less volatile content of the GY anthracite, almost no hydrocarbons are generated in the combustion process, and the overall performance is the combustion reaction of char. Therefore, the ignition location of the GY-coal can be judged by the char thermal radiation signal instead, which attains 32 ms in the image.

The right side of Fig. 4 shows that the ignition location of single pulverized coal particles is significantly advanced when NH_3 carries the pulverized coal into the high temperature and thermal environment. It is because the pre-combustion of NH_3 flame greatly increases the temperature of the flue gas around coal, promotes the early release of volatiles in single coal particles, and thus accelerates the ignition process. When carried by NH_3, single particles of XM-coal ignite on fire at 12 ms. The boundary line between the volatile gas flame and heterogeneous char combustion is no longer evident, and the ignition mode changes to homogeneous-heterogeneous united ignition [31]. The rate of fragmentation occurring during heat-up and devolatilization could affect overall particle burning rates, as reported by Mitchell and Akatenuk [32]. Such fragmentation of coal particles can be observed frequently under the NH_3 atmosphere. The single particles of IM-coal and ZD-coal ignite at around 16 ms and 20 ms, respectively, accompanied by greatly enhanced CH* signal intensity, indicating that the combustion reaction is both speed up and enhanced significantly under the NH_3 atmosphere. As for GY-coal, the ignition position moves forward at ~20 ms under NH_3 carrying condition.

It should be noted that even for the same type of coal, the microstructure and chemical composition of every single particle cannot be entirely consistent at the individual level, so the characteristics and phenomena in the combustion process are bound to be slightly different. Hence, the experiments were repeated 20 times for each case, and the signal distributions of the single particle ignition process were counted by average, which allowed the collected results with statistical significance. The statistical average conclusions are given in Section 3.2.2 below.

3.2. Ignition and combustion processes

3.2.1. Temporally resolved images of single particle ignition in the N_2/NH_3 atmosphere

The typical temporally resolved CH* chemiluminescence (XM/IM/ZD-coal) and char thermal radiation (GY-coal) signals of single burning particles under N_2 (1~4) and NH_3 (5~8) atmosphere with O_2 content in the background flue gas of 20 % are shown in Fig. 5(a). It is observed that the ignition and combustion characteristics of the tested coals with different ranks exhibited distinct features, which explicitly means different ignition modes, ignition delay times and volatile burnout times.

According to Fig. 5, the initial ignition positions of four coal samples delay successively with the increase of coal rank, starting from 15 mm HAB (height above the burner) to 25 mm HAB. As the low-rank coal with high volatile content, XM lignite (case 1) started homogeneous ignition at ~24 ms, and the combustion of volatiles lasted ~8 ms. Then, the heterogeneous oxidation of the residual char occurred at 44 ms, along with the remaining volatiles release and burning. However, with the increase of coal rank, the initial position of CH* signals appeared later around 28~30 ms for IM-coal (case 2) and ZD-coal (case 3) and the transition region where signal intensities suddenly drop could no longer be observed. Hence, these cases were classified as heterogeneous ignition mode. As for GY anthracite (case 4), characterized by the char thermal radiation signal at 850 nm band, did not occur heterogeneous ignition until 32 ms, and the signal intensities were feeble. The ammonia blended combustion cases (5~8) are shown on the right side of Fig. 5(a). Compared with the height of the NH_3 flame on the right, we can observe that the single coal particle immediately ignited within the area of the NH_3 flame. Therefore, the ignition delay time was considerably shortened. In the meantime, the CH* signal intensities were significantly increased. These divergences indicate that adding NH_3 would promote the devolatilization reaction and accelerate the ignition process for single coal particles. From the perspective of ignition mode, when the central nitrogen flow is replaced by NH_3/N_2, the ignition modes of coal particles have some changes: the volatile gaseous flame area increased for XM-coal, and CH* signals appeared earlier (within 16~24 ms) in the ignition process for IM-coal and ZD-coal. The above changes indicate that: in the NH_3 atmosphere, the homogeneous ignition characteristics

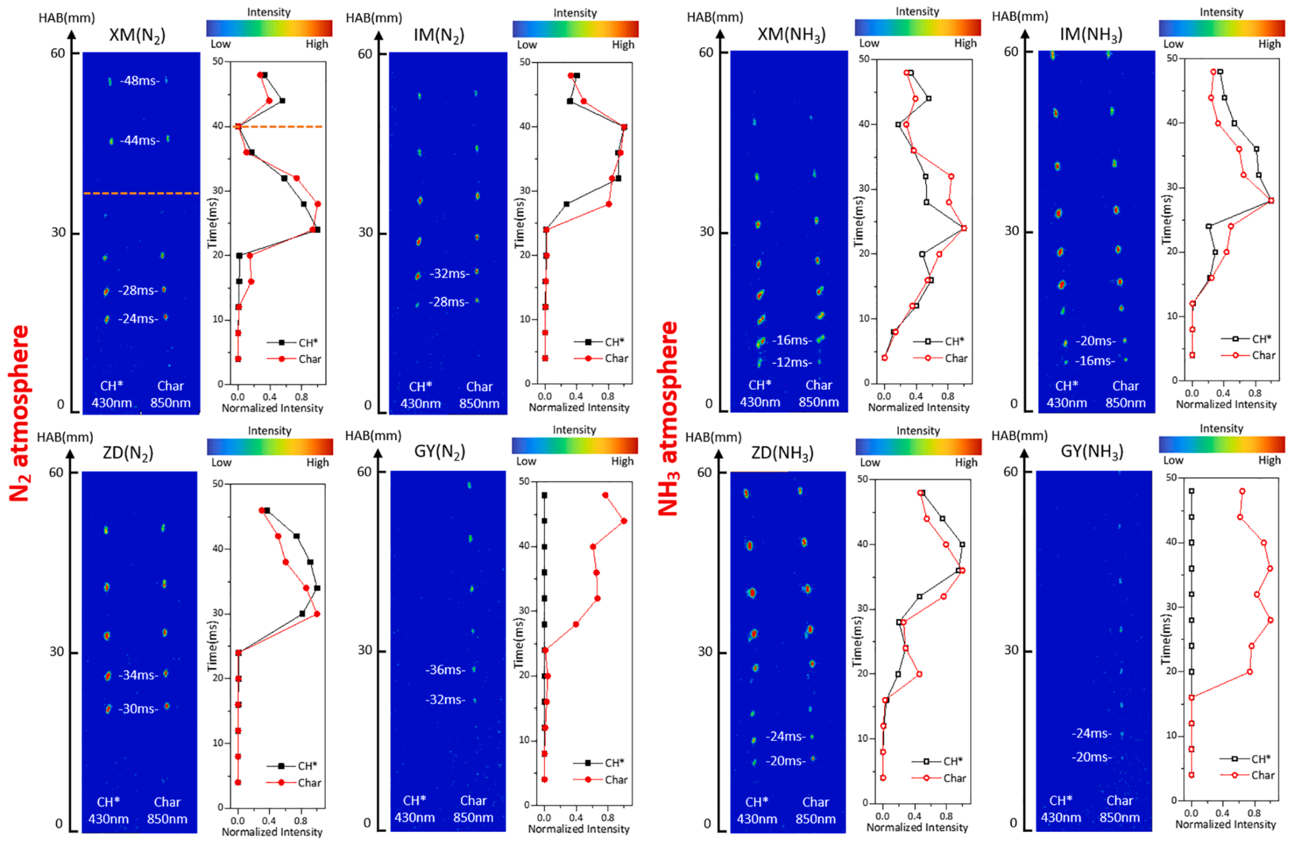

Fig. 4. CH*/char images and signal intensity profile of typical coal single particles combustion.

of XM-coal particles are strengthened with the overlap of homogeneous and heterogeneous ignition zones, while the IM-coal and ZD-coal particles showed a transitional trend from the heterogeneous ignition mode to the homogeneous-heterogeneous united ignition mode, where a new signal peak appears in the early stage of the CH* intensity profile.

The normalized CH*/Char signal intensity profiles in the N_2 and NH_3/N_2 atmospheres are shown in Fig. 5(b), which is directly converted from Fig. 5(a). By comparing line 1) and line 5), we can see that the CH* intensity of the XM-coal particle presents a bimodal distribution along with the residence time under both nitrogen and NH_3 atmospheres. The first signal peak at 25 ms represents the gaseous flame where homogeneous volatile ignition happens. The second peak at 45 ms represents the gas-solid two-phase flame where heterogeneous char oxidation occurs. Therefore, the minimum between 35∼40 ms indicates the extinguishing of the volatile gaseous flame and the beginning of the heterogeneous char ignition. Such bimodal distribution behavior also exists in the NH_3 atmosphere, with the minimum intensity advanced to ∼20 ms. By comparing line 2) and line 6), we can find that the CH* intensity curve of the IM-coal transforms from the unimodal distribution to the bimodal distribution when NH_3 is blended. The inflexion point appears at 25 ms, and the signal peak moves forward. Such transition indicates that the ignition behavior gradually changes from heterogeneous ignition to homogeneous ignition when the primary air is replaced from N_2 to NH_3. As for ZD-coal (lines 3, 7) and GY-coal (lines 4, 8), the flame signals present unimodal distribution without noticeable turning points, which means their particle ignition processes keep still as heterogeneous ignition modes. To sum up, replacing the primary air from N_2 with NH_3 will lead to the evolution of the normalized CH* signal intensity from unimodal distribution to bimodal distribution for partial single coal particles and significantly advance the occurrence location of the CH* chemiluminescence and char thermal radiation, which would shorten the ignition delay time as is well-known.

3.2.2. Statistical results of CH* chemiluminescence and char thermal radiation intensity during ignition

The average statistical results of CH* (XM/IM/ZD-coal) and char (GY-coal) signal intensity variations as a function of residence time in the N_2 and NH_3 carrying conditions (20 images counted for each case) are shown in Fig. 6. Based on the signal heights of the curves in Fig. 6(a) and (b), the intensities of CH* chemiluminescence and char thermal radiation signals significantly increased when N_2 is replaced by NH_3, which directly confirms the enhancement effect of NH_3 addition on the devolatilization and combustion of single coal particles. Such enhancement can be explained by the following reasons: (1) In the high-temperature background flue gas around 1550 K, the NH_3-carrying gas in the central jet rapidly burned once it entered the hot environment. Therefore, the ambient temperature around the coal particles in the ammonia-doped condition is significantly higher than the N_2 carrying case. The heat emitted from NH_3 flame (located ∼10 mm HAB) increased the particle devolatilization and combustion reaction rate, which led to the ignition in advance; (2) The molecules and active radicals (e.g. H, NH, NH_2) decomposed from NH_3 could react with the volatile matters, which causes the in advance of the particle ignition and facilitates the process of coal combustion.

In order to determine the characteristic ignition times, Fig. 7 shows the normalized chemiluminescence signal intensity as a function of the residence time based on Fig. 6. In previous studies, two main ways exist to define the ignition delay time. Riaza et al. [22] measured the temperature temporal evolution of the burning particles, and defined the ignition temperature as the first point where the particle temperature gradient reached the maximum. Simoes et al. [33] concluded that 15 % of the maximum luminosity intensity is a more consistent ignition criterion for single-particle ignition events. Similarly, Qi et al. [28] and Weng et al. [29,30] also took 15 % of the maximum CH* chemiluminescence signal intensity as the ignition criterion for single coal and biomass particles and found that the results agreed well with the

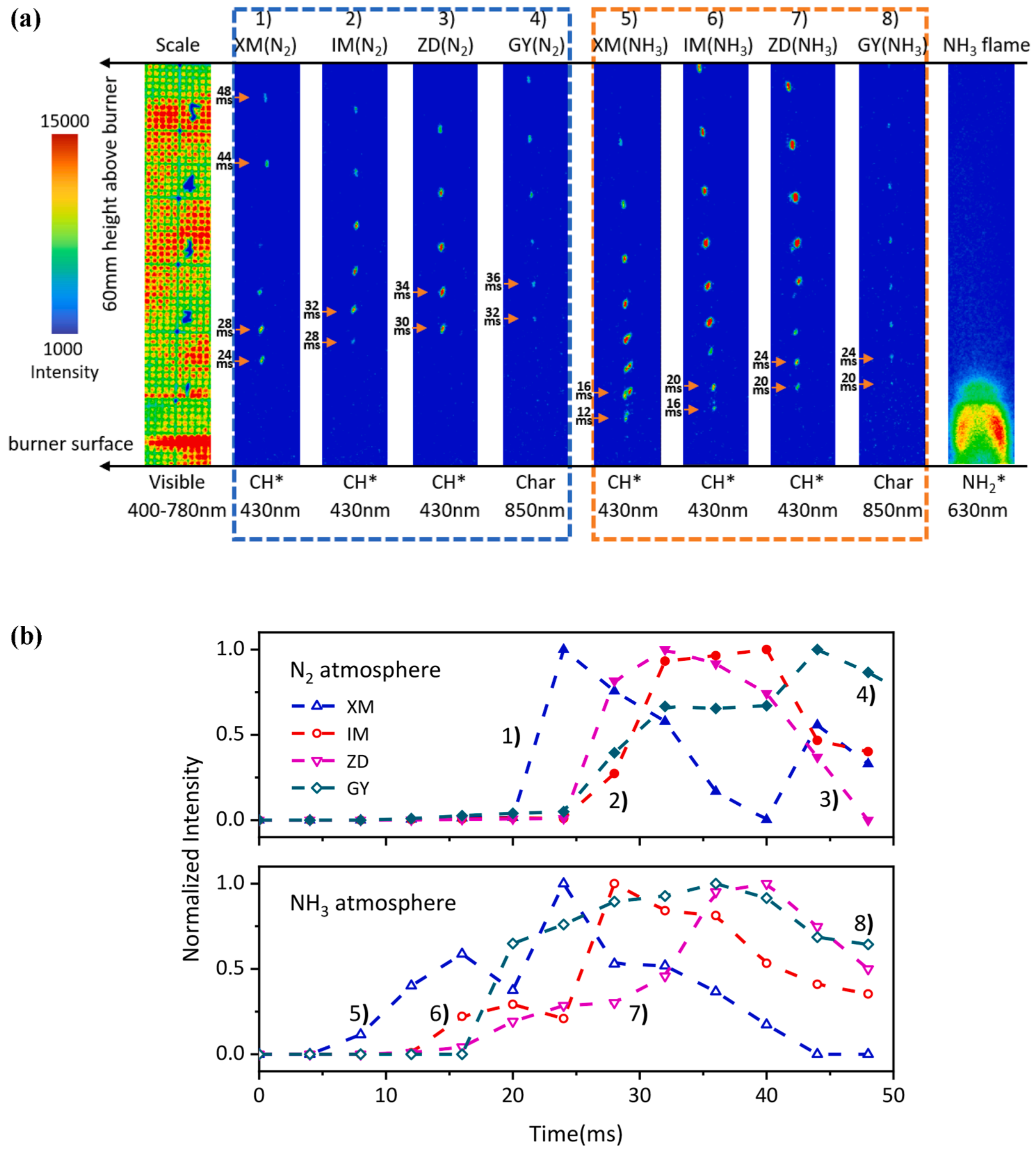

Fig. 5. Temporally resolved chemiluminescence images of single particles combustion in the N_2/NH_3 atmospheres and the corresponding normalized CH*/Char signal intensity profiles.

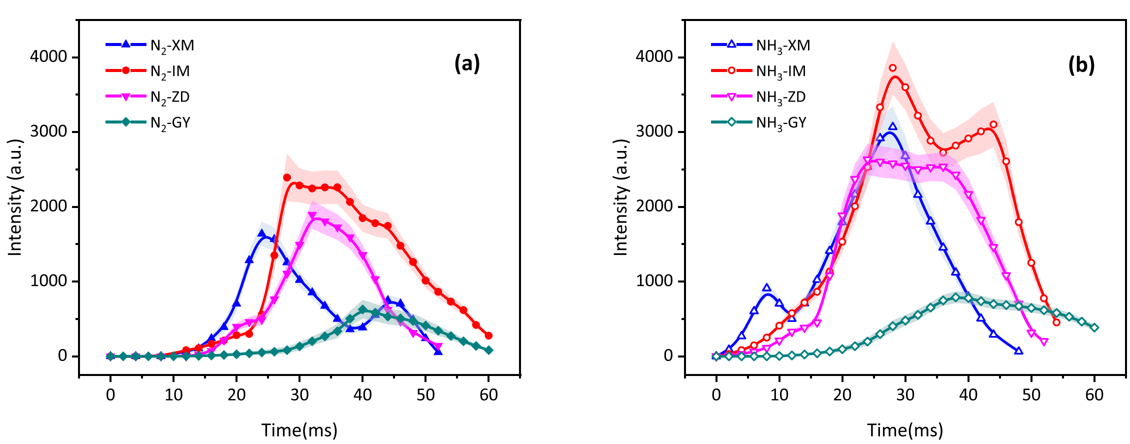

Fig. 6. Statistical chemiluminescence signal intensity as a function of the residence time in the (a) N_2 and (b) NH_3 atmospheres with 95 % confidence level.

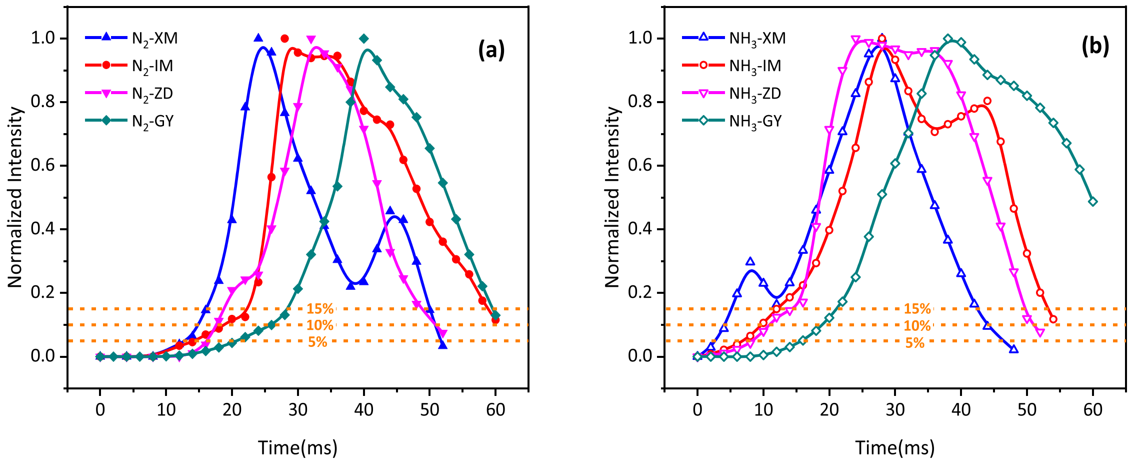

Fig. 7. Normalized statistical chemiluminescence signal intensity as a function of the residence time in the (a) N_2 and (b) NH_3 atmospheres.

ignition delay time calculated by the max-gradient method. This study adopted the second method (15 % of the maximum normalized chemiluminescence intensity) and plotted the baselines of 5, 10 and 15 % of normalized CH*/Char intensities in Fig. 7. It can be seen that the baseline of 15 % shows better distinction for different coal types than other two baselines and thus it is used as the discrimination criterion in the following discussions.

3.3. Characteristic time of the single particle ignition process

Based on the above illustration, the 15 % of the maximum normalized chemiluminescence intensity was used as the criterion to determine the beginning and ending of the combustion of single coal particles. Accordingly, the characteristic times throughout the whole combustion process are defined as follows in Fig. 8:

(1) Ignition delay time (IDT), which ranges from 0 ms to the first intersection point of signal intensity curve and the baseline. It characterizes how fast the particle begins to ignite.
(2) Interval from ignition to peak intensity (ITP), which ranges from the first intersection point to the timing of the maximum signal intensity. It describes how much time the particle would experience since ignition until the coal combustion comes to the most intense moment.
(3) Combustible component burnout time (CBT), which ranges from the first intersection of the intensity curve and the baseline to the last intersection. It indicates how long the whole combustion process could last, including the volatiles combustion stage and the char combustion stage.

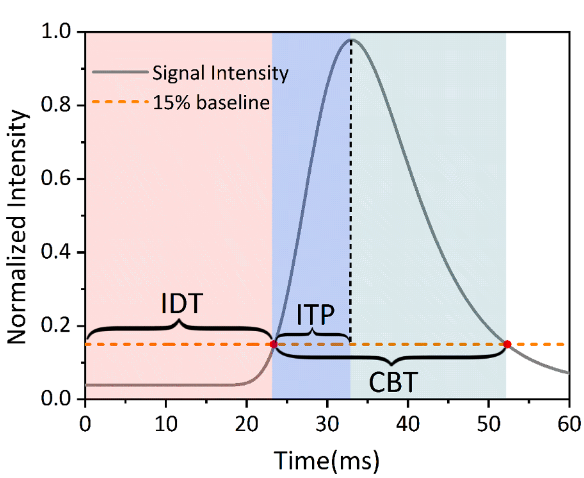

Fig. 8. Characteristic time (IDT, ITP and CBT) definition.

3.3.1. Ignition delay time (IDT)

The ignition delay time (IDT) obtained through the 15 % baseline for different coal types in the N_2 and NH_3 atmospheres are shown in Fig. 9, the data are obtained from Fig. 7. The volatile matter contents of each coal type are plotted as grey dots on the right axis. From the perspective of fuel properties, the ignition delay times of single coal particles generally present monotonously upward trends with the decrease of volatile matter content, e.g. lignite (XM) $<$ bituminous (IM/ZD) $<$anthracite (GY). It is understandable since the ignition delay time for coal particles are closely related to their volatile contents. In addition, the change of the thermal environment surrounding coal particles will affect the heat transfer, mass transfer and reaction characteristics of the combustible components, which further influence the ignition behaviors of single coal particles. Specifically, when N_2 is replaced with NH_3 in the carrier gas flow, significant decreases of the IDTs can be observed among the coal samples. As the arrows marked, the IDTs decreased by 7.9 ms (XM), 10.5 ms (IM), 4.4 ms (ZD) and 7.4 ms (GY), respectively.

Based on the present statistical results, when coal particles were carried by NH_3 atmosphere, the XM particles ignited homogeneously at ~8 ms, the IM and ZD particles ignited at 12~14 ms, and GY particles ignited heterogeneous at ~21 ms. Since the divergencies of the background gas, jet velocity, temperature, burner structure and other factors, it is hard to directly compare the experimental data of relevant studies [16,19,22,23,34]. Nevertheless, the IDT levels are all within the range of

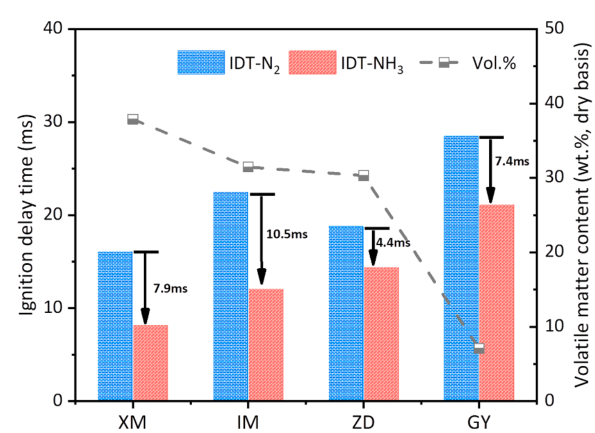

Fig. 9. Ignition delay time for different coal types in the N_2 and NH_3 atmospheres, as compared with the volatile matter content.

10~100 ms, as same as this research. Moreover, our previous work obtained consistent descending tendencies of single-particle IDTs with increased volatile content in the N_2/CO_2 environments [28].

3.3.2. Interval from ignition to peak intensity (ITP)

After ignition, the combustion reactions of coal particles accelerate rapidly, and the flame chemiluminescence signal intensity rises continuously. The time interval from ignition to peak CH*/char signal intensity (ITP) for different coal types in the N_2 and NH_3 atmospheres are shown in Fig. 10 with data obtained from Fig. 7. The CH*/char signal intensity here represents the combustion rate of the particles' volatile. In the N_2 atmosphere, XM and IM particles with high volatile content reach the peak combustion rate at ~8.5 ms and ~6.2 ms after ignition, respectively. As for ZD and GY particles with high fixed carbon content, it takes longer time (13.7 ms and 12.1 ms, respectively).

Concerning the NH_3 atmosphere, the ITP intervals for all coal types improve conformably. On the one hand, it is because of the IDT for coal particles being advanced with NH_3 flame preheated. On the other hand, the peak position of the chemiluminescence signal moves backwards due to NH_3 carrying, especially for XM and IM particles. As shown in Fig. 5(a) above, the coal combustion with NH_3 carrying is more intense, and the chemiluminescence signal peaks of XM and IM coal postpone from the homogeneous burning region (upstream) to the homogeneous-heterogeneous united burning region (downstream). Therefore, the ITP of these two coal particles increase significantly (11 ms and 9.7 ms, respectively), which indicates that the durations of high-intensity combustion are prolonged.

3.3.3. Combustible component burnout time (CBT)

As discussed earlier (cf. Fig. 5), the devolatilization of the coal particles can occur during the pre-ignition stage, the volatile combustion process, and the char oxidation stage. The volatile combustion and char oxidation stages overlap for the particles experiencing heterogeneous ignition and combustion. The time interval between the two intersections of the 15 % baseline and normalized intensity curve in Fig. 7 is defined as the combustible component burnout time (CBT) following the related literature [28]. Fig. 11 shows the CBT for four types of coal particles in the N_2 and NH_3 atmospheres. As illustrated by the arrows, when N_2 is replaced with NH_3 in the carrier gas, the CBT values for all coal types extend by 3~6 ms. Two main reasons can be concluded: Firstly, the NH_3 flame promotes the devolatilization of particles and accelerates the temperature rise to ignition, which moves forward the starting position; Secondly, the coal combustion period is prolonged in the presence of NH_3, which lengthens the duration time from ignition to burnout.

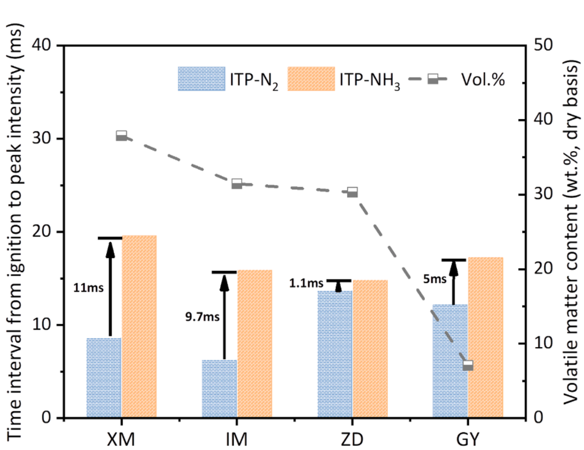

Fig. 10. Interval from ignition to peak intensity of chemiluminescence signal for different coal types in the N_2 and NH_3 atmospheres, as compared with the volatile matter content.

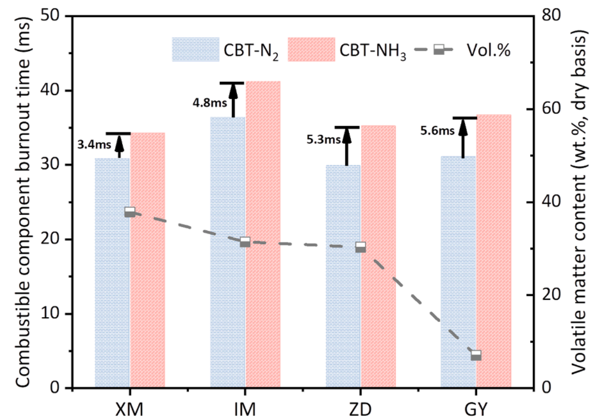

Fig. 11. Combustible component burnout time for different coal types in the N_2 and NH_3 atmospheres, as compared with the volatile matter content.

3.4. Effect of O_2 content in flue gas on ammonia/coal single particle ignition delay time

The CH*/char signal images of the single coal particles under different O_2 content (10, 20, 30 %) in the background flue gas are shown in Fig. 12, compared with the NH_3 flame height on the left. In terms of characteristic time, as O_2 content changes from 10 to 30 %, the location of ignition occurring moves forward in order, which means the ignition delay time shortens. In addition, the signal intensities of the CH*/char are significantly enhanced, indicating that the volatile oxidation and char burning intensity increase dramatically, no matter in the N_2 or NH_3 atmosphere.

From the perspective of ignition mode, XM particles generally present the characteristics that gas-phase ignition and volatile combustion occur prior to heterogeneous oxidation under various O_2 content. The homogeneous-heterogeneous transition region where CH* chemiluminescence disappears can be observed distinctly in the upper-left of Fig. 12. Concerning ammonia-blended cases, the NH_3 flow heats the single particle intensively, which contributes to the quick release of volatiles and burning. Meanwhile, the elevated temperature shortens the heat transfer process from the surface to the interior of particles and enhances the char's chemical reactivity, significantly bringing forward the heterogeneous combustion time. Therefore, the transition region of XM particles may vanish in the NH_3 carrying cases (e.g. 20 % O_2 content). IM and ZD particles generally present heterogeneous ignition characteristics and tend to ignite in homogeneous-heterogeneous united mode when O_2 content exceeds 20 %. Unsurprisingly, GY particles keep the typical heterogeneous ignition characteristics in all cases since they almost contain no volatilities.

The ignition delay time (IDT) variation for XM, IM, ZD and GY particles under different O_2 content (10 %/20 %/30 %) and carrier gas (N_2/NH_3) atmosphere are shown in Fig. 13. No matter in the N_2 or NH_3 atmosphere, the IDT curves for all coal types reveal monotonously decreasing trends with the increase of the O_2 content. That is to say, the oxygen-enriched strategy can be applied into both pure coal combustion and ammonia/coal co-firing occasions to effectively shorten the ignition process and increase the burning rates at the single-particle scale.

4. Conclusions

This study investigated the ignition and combustion characteristics of ammonia/coal co-firing conditions under different coal types, O_2 content and carrier gas conditions. The CH*/Char chemiluminescence signal intensity distribution and ignition characteristic time of single coal particles in both N_2 and NH_3 atmospheres were obtained. The new findings are summarized below:

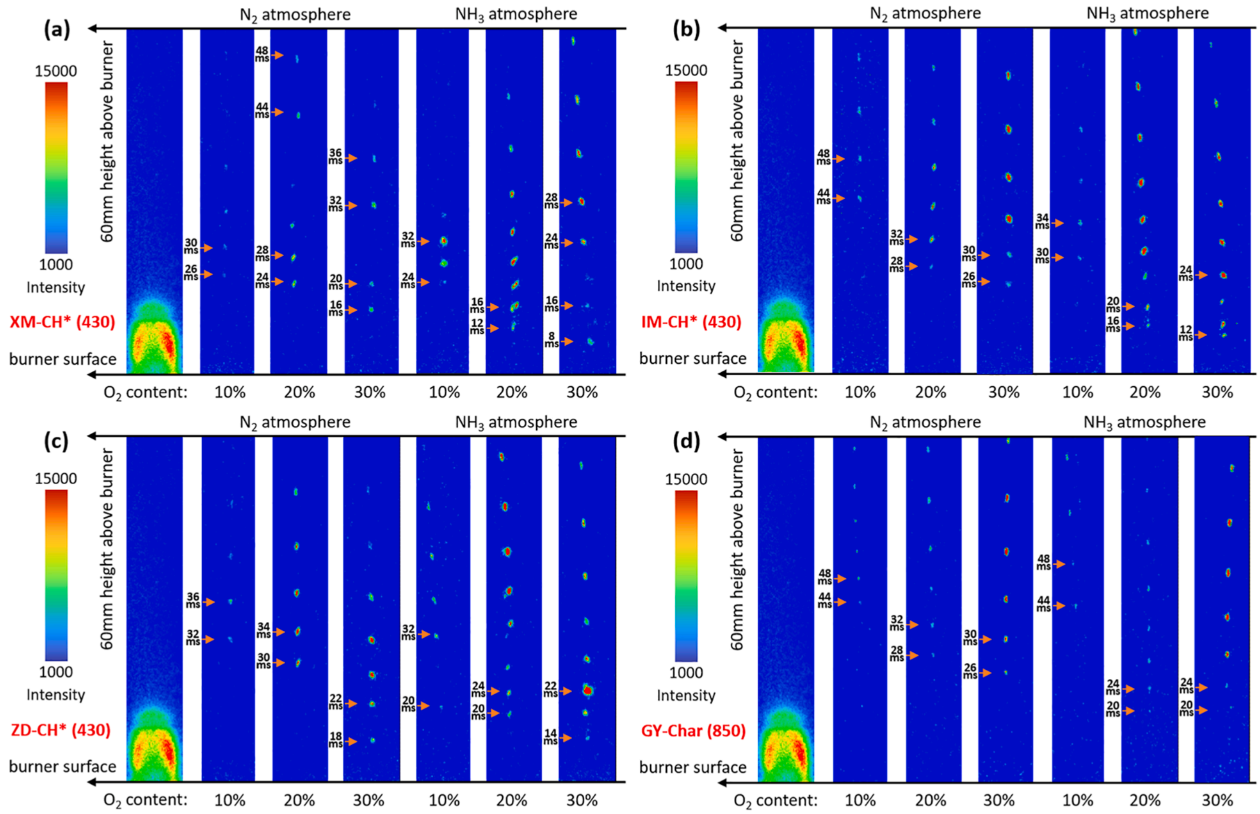

Fig. 12. Chemiluminescence images of single particles combustion with different O_2 content (10~30 %).

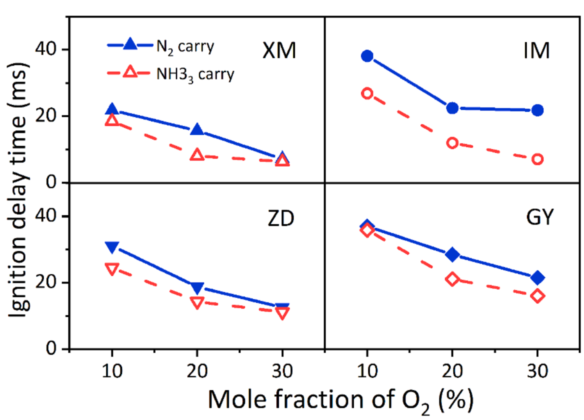

Fig. 13. Ignition delay time variation with different O_2 content and carrier gas (N_2/NH_3) atmosphere for XM, IM, ZD and GY coal samples.

(1) In ammonia co-firing condition, with the carrier gas was replaced by NH_3, the ignition delay time of all coal particles was greatly shortened. The ignition delay time was significantly influenced by coal rank, e.g. lignite < bituminous <anthracite, as observed in the present work. Meanwhile, the CH* signal intensities were significantly enhanced. These results indicated that the co-firing of NH_3 can promote the devolatilization process of coal particles and accelerate the initiation of ignition behavior.

(2) In normal combustion condition, with the N_2 as carrier gas, an obvious signal peak can be observed in the early stage of the normalized CH* intensity profile of XM-coal, while the single-particle ignition of IM/ZD/GY-coal were dominated by the heterogeneous ignition mode and the chemiluminescence curves showed unimodal distribution. In the NH_3 co-firing conditions, the homogeneous ignition behaviors of the XM particles are further enhanced, and the IM and ZD particles shift to the homogeneous-heterogeneous united ignition mode.

(3) With the increase of O_2 content, no matter with or without ammonia addition, the ignition positions advanced orderly, the ignition delay time shortened monotonously, and the chemiluminescence intensity increased significantly, which indicate that the oxidation and burning rates of volatiles and the combustion intensity of char are notably improved.

Declaration of competing interest

The authors declare that they have no known competing financial interests or personal relationships that could have appeared to influence the work reported in this paper.

Acknowledgments

This work was supported by the National Natural Science Foundation of China (52125605), the National Key R&D Program of China (2022YFB4003902) and the Fundamental Research Funds for the Central Universities (2022ZFJH04).

Supplementary materials

Supplementary material associated with this article can be found, in the online version, at doi:10.1016/j.combustflame.2024.113385.

References

[1] A. Yapicioglu, I. Dincer, A review on clean ammonia as a potential fuel for power generators, Renew. Sustain. Energy Rev. 103 (2019) 96–108.
[2] T. Yoshizaki, Test of the co-firing of ammonia and coal at mizushima power station, Ki. Aika, H. Kobayashi (Eds.). CO_2 Free Ammonia as an Energy Carrier: Japan's Insights, Springer Nature Singapore, Singapore, 2023, pp. 601–611.

[3] JERA and IHI to start a demonstration project related to ammonia co-firing at a large-scale commercial coal-fired power plant. https://www.jera.co.jp/english/information/20210524_677.
[4] T. Niu, W. Zhang, X. Liu, D. Hu, T. Wang, Y. Xie, H. Wang, Industrial-scale experimental investigation of ammonia-coal cofiring in coal-fired boiler, Clean Coal Technol. 28 (2022) 193–200.
[5] Y. Xia, K. Hadi, G. Hashimoto, N. Hashimoto, O. Fujita, Effect of ammonia/oxygen/nitrogen equivalence ratio on spherical turbulent flame propagation of pulverized coal/ammonia co-combustion, Proc. Combust. Inst. 38 (2021) 4043–4052.
[6] K. Hadi, R. Ichimura, G. Hashimoto, Y. Xia, N. Hashimoto, O. Fujita, Effect of fuel ratio of coal on the turbulent flame speed of ammonia/coal particle cloud co-combustion at atmospheric pressure, Proc. Combust. Inst. 38 (2021) 4131–4139.
[7] J. Zhang, T. Ito, H. Ishii, S. Ishihara, T. Fujimori, Numerical investigation on ammonia co-firing in a pulverized coal combustion facility: effect of ammonia co-firing ratio, Fuel 267 (2020).
[8] M. Tamura, T. Gotou, H. Ishii, D. Riechelmann, Experimental investigation of ammonia combustion in a bench scale 1.2MW-thermal pulverised coal firing furnace, Appl. Energy 277 (2020).
[9] H. Lee, M.J. Lee, Recent advances in ammonia combustion technology in thermal power generation system for carbon emission reduction, Energies 14 (2021).
[10] T. Ito, J. Zhang, H. Ishii, T. Suda, T. Fujimori, Development of pulverized coal/ammonia co-firing technology, Ki. Aika, H. Kobayashi (Eds.). CO_2 Free Ammonia as an Energy Carrier: Japan's Insights, Springer Nature Singapore, Singapore, 2023, pp. 591–599.
[11] E. Marek, K. Stańczyk, Case studies investigating single coal particle ignition and combustion, J. Sustain. Min. 12 (2013) 17–31.
[12] A. Molina, C.R. Shaddix, Ignition and devolatilization of pulverized bituminous coal particles during oxygen/carbon dioxide coal combustion, Proc. Combust. Inst. 31 (2007) 1905–1912.
[13] C.R. Shaddix, A. Molina, Particle imaging of ignition and devolatilization of pulverized coal during oxy-fuel combustion, Proc. Combust. Inst. 32 (2009) 2091–2098.
[14] X. Bai, G. Lu, T. Bennet, A. Sarroza, C. Eastwick, H. Liu, Y. Yan, Combustion behavior profiling of single pulverized coal particles in a drop tube furnace through high-speed imaging and image analysis, Exp. Therm. Fluid Sci. 85 (2017) 322–330.
[15] R. Khatami, Y.A. Levendis, On the deduction of single coal particle combustion temperature from three-color optical pyrometry, Combust. Flame 158 (2011) 1822–1836.
[16] R. Khatami, Y.A. Levendis, An overview of coal rank influence on ignition and combustion phenomena at the particle level, Combust. Flame 164 (2016) 22–34.
[17] R. Khatami, Y.A. Levendis, M.A. Delichatsios, Soot loading, temperature and size of single coal particle envelope flames in conventional- and oxy-combustion conditions (O_2/N_2 and O_2/CO_2), Combust. Flame 162 (2015) 2508–2517.
[18] R. Khatami, C. Stivers, K. Joshi, Y.A. Levendis, A.F. Sarofim, Combustion behavior of single particles from three different coal ranks and from sugar cane bagasse in O2/N2 and O_2/CO_2 atmospheres, Combust. Flame 159 (2012) 1253–1271.
[19] R. Khatami, C. Stivers, Y.A. Levendis, Ignition characteristics of single coal particles from three different ranks in O_2/N_2 and O_2/CO_2 atmospheres, Combust. Flame 159 (2012) 3554–3568.
[20] Y.A. Levendis, K. Joshi, R. Khatami, A.F. Sarofim, Combustion behavior in air of single particles from three different coal ranks and from sugarcane bagasse, Combust. Flame 158 (2011) 452–465.
[21] T. Maffei, R. Khatami, S. Pierucci, T. Faravelli, E. Ranzi, Y.A. Levendis, Experimental and modeling study of single coal particle combustion in O_2/N_2 and Oxy-fuel (O_2/CO_2) atmospheres, Combust. Flame 160 (2013) 2559–2572.
[22] J. Riaza, R. Khatami, Y.A. Levendis, L. Álvarez, M.V. Gil, C. Pevida, F. Rubiera, J. J. Pis, Single particle ignition and combustion of anthracite, semi-anthracite and bituminous coals in air and simulated oxy-fuel conditions, Combust. Flame 161 (2014) 1096–1108.
[23] R.B. Kops, F.M. Pereira, M. Rabaçal, M. Costa, Effect of steam on the single particle ignition of solid fuels in a drop tube furnace under air and simulated oxy-fuel conditions, Proc. Combust. Inst. 37 (2019) 2977–2985.
[24] J. Köser, L.G. Becker, A.K. Goßmann, B. Böhm, A. Dreizler, Investigation of ignition and volatile combustion of single coal particles within oxygen-enriched atmospheres using high-speed OH-PLIF, Proc. Combust. Inst. 36 (2017) 2103–2111.
[25] Y. Yuan, S. Li, G. Li, N. Wu, Q. Yao, The transition of heterogeneous–homogeneous ignitions of dispersed coal particle streams, Combust. Flame 161 (2014) 2458–2468.
[26] Y. Yuan, S. Li, Y. Xu, Q. Yao, Experimental and theoretical analyses on ignition and surface temperature of dispersed coal particles in O_2/N_2 and O_2/CO_2 ambients, Fuel 201 (2017) 93–98.
[27] Y. Yuan, S. Li, F. Zhao, Q. Yao, M.B. Long, Characterization on hetero-homogeneous ignition of pulverized coal particle streams using CH* chemiluminescence and 3 color pyrometry, Fuel 184 (2016) 1000–1006.
[28] S. Qi, Z. Wang, M. Costa, Y. He, K. Cen, Ignition and combustion of single pulverized biomass and coal particles in N_2/O_2 and CO_2/O_2 environments, Fuel 283 (2021).
[29] W. Weng, M. Costa, M. Aldén, Z. Li, Single particle ignition and combustion of pulverized pine wood, wheat straw, rice husk and grape pomace, Proc. Combust. Inst. 37 (2019) 2663–2671.
[30] W. Weng, M. Costa, Z. Li, M. Aldén, Temporally and spectrally resolved images of single burning pulverized wheat straw particles, Fuel 224 (2018) 434–441.
[31] H. Jüntgen, K.H. Van Heek, An update of german non-isothermal coal pyrolysis work, Fuel Process. Technol. 2 (1979) 261–293.
[32] R.E. Mitchell, A.E.J. Akanetuk, The impact of fragmentation on char conversion during pulverized coal combustion, Symp. Int. Combust. 26 (1996) 3137–3144.
[33] G. Simões, D. Magalhães, M. Rabaçal, M. Costa, Effect of gas temperature and oxygen concentration on single particle ignition behavior of biomass fuels, Proc. Combust. Inst. 36 (2017) 2235–2242.
[34] D. Magalhães, F. Kazanç, A. Ferreira, M. Rabaçal, M. Costa, Ignition behavior of Turkish biomass and lignite fuels at low and high heating rates, Fuel 207 (2017) 154–164.